H_2O contents and hydrogen isotopic composition of apatite crystals from L, LL5-6 ordinary chondrites.

K. Yanai[1] , S. Itoh[1], J. P. Greenwood[2] and H. Yurimoto[1], [1]Dept Natural History Sciences, Hokkaido University 060-0810, Japan. [2]Dept Earth & Environmental Sciences, Wesleyan Univ., 265 Church street, Middletown, Conneticut 06459, USA. e-mail to: kaori@ep.sci.hokudai.ac.jp

Introduction: Ordinary chondrites of petrologic types 4 to 6 exhibit a sequence of progressive chemical and textural equilibration, and contain Cl-rich apatite grains [1-3].

Previous study reported that the water contents of chlorapatite are very low (<100ppm), even though apatite grains in ordinary chondrites seem to have a significant H_2O contents based on a deficit of anions [3]. As results, they suggest that apatite grains were formed with a dry and halogen-bearing fluid that has been derived by degassing of chondritic melts.

However, the condition of fluids is still unclear, because boundaries between the phosphate mineral and the olivine in St. Séverin (LL6) appear to consist of a diffuse reaction zone, <1 μm across but there is no similar texture from LL4-5 OCs [4]. This shows that the different types of fluids are resulting from the crystallization of apatite.

In this study, we report the petrography, H_2O contents and hydrogen isotopic compositions in chlorapatite with and without this reaction texture from L, LL5-6 ordinary chondrites using secondary ion mass spectrometry (SIMS) to estimate these various fluids for the apatite grains.

Analytical methods: Thick section (Mocs (L5-6), Ensisheim (LL6)) mounted one inch with San Carlos Olivine was used in this study. Apatite grains were identified using elemental X-ray mapping using scanning electron microscope (FE-SEM JEOL JSM 7000-F) and energy dispersive X-ray spectrometry (EDS Oxford INCA Energy) at Hokkaido University (Fig. 1). Quantitative analyses were also performed using FE-SEM-EDS system.

A $^{133}Cs^+$ primary beam of 20 keV was focused to a beam spot of ~20 μm on the surface of the

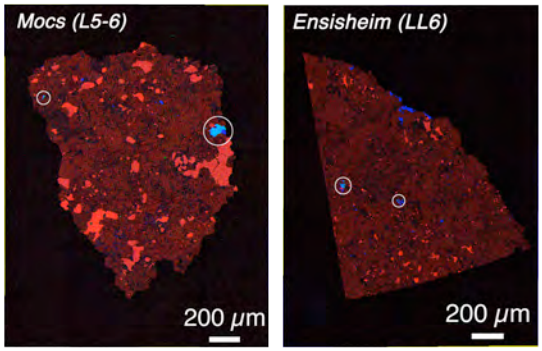

Fig. 1. X-ray mapping of Mocs and Ensisheim. RGB map to identified apatite and merrillite. White circles denote the apatite grains. R; F, G; Cl B; P.

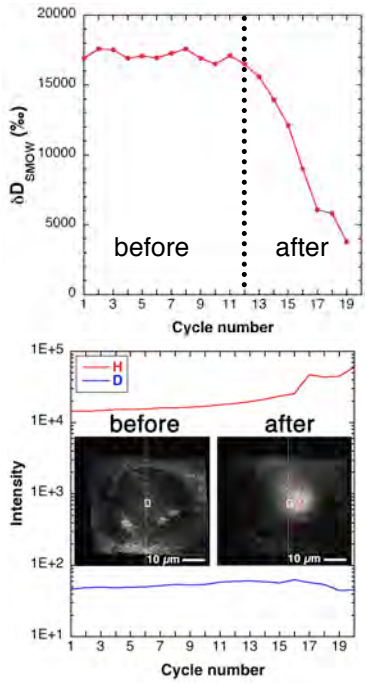

Fig. 2. The secondary ion intensity of hydrogen vs. cycles and δD vs. cycles by SIMS. The dashed line shows the starting cycle of crack. The secondary hydrogen images before and after appearing cracks are shown.

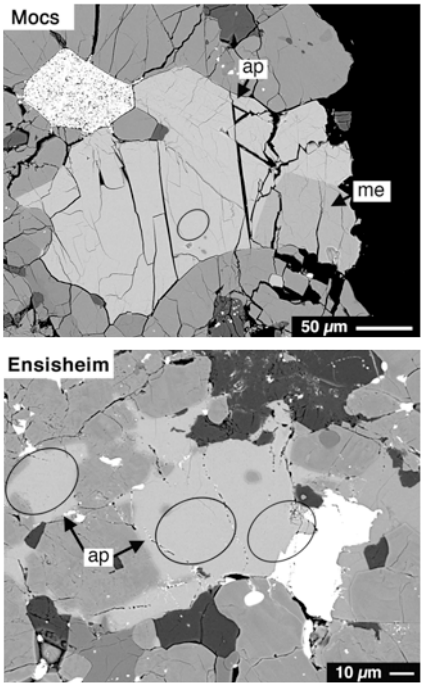

Fig. 3. BSE images of apatite grains in Mocs and Ensisheim. Circles show the SIMS spots. Ap = apatite. Me = merrillite.

sample with a beam current of ~15 nA. In order avoid crater edge effects and adsorbed water on the surface, a relatively large primary beam was used, and secondary ions generated from the center of the primary beam irradiation area of 2 x 2 μm^2 were collected using a field aperture. The intense primary beam used is very effective for improving the detection limit of sample hydrogen under SIMS analysis [5]. We carefully selected analysis positions using stigmatic imaging to avoid water contamination, such as along grain boundaries, cracks and micro-cracks. We sometimes observed a sudden increase of the hydrogen secondary ion signal during a measurement (Fig. 2). This is due to the encounter of water contamination at depth during the excavation of the sputtered crater. In these cases, we immediately evaluated the reason for the sudden increase in secondary hydrogen intensity by ^1H imaging (as described above) and rejected the disturbed data.

The Durango apatite (0.0478 wt%) and Linopolis apatite (1.28 wt%) were used to estimate the H_2O content using the calibration curve with $H/^{18}O$ ratio. In the same analytical session, the $H/^{18}O$ ratio of San Carlos olivine crystal (20 ppm: [6]) was also used as a standard with assumption of similar matrix effect of chlorapatite. Negative secondary ions of ^1H and D were collected sequentially in an electron multiplier on the optical axis for 2 seconds and for 20 seconds, respectively, in peak-jumping mode, at a mass resolving power M/ΔM about 2000. The hydrogen isotopic compositions of apatite were calculated using Durango apatite (δD_{SMOW} = –121‰) and that of olivine using San Carlos olivine (δD_{SMOW} = 0‰). The overall analytical errors (2σ) were about 20‰ in apatite and 150‰ in olivine. The other detail analytical conditions are shown in [7].

Results and discussions: All apatite grains from two ordinary chondrites are determined as chlorapatite grains. Two chlorapatite grains from Mocs and Ensisheim were measured H_2O contents and hydrogen isotopic compositions by SIMS (Fig. 3). Remarkably, chlorapatite grains in Ensisheim show a similar reaction texture [4], which boundaries between the apatite and the olivine appear to consist of a diffuse reaction zone (Fig. 4).

The H_2O contents of apatite grains in Ensisheim (LL6) and Mocs (L5-6) are estimated to be ~60 ppm and ~35 ppm, respectively. These H_2O contents are similar to the previous reported values from LL chondrites [3]. The hydrogen isotopic compositions of apatite grains from Ensisheim are extremely D-rich (δD= ~ +17000‰). The degassing of OH from apatite grains is resulting from D-poor signature [8]. Therefore, the D-rich signature of Ensisheim apatite must be resulting from D-rich fluids. These results indicate that the different hydrogen isotopic compositions of fluids existed in L, LL ordinary chondrites parent body, even if it is unclear about the origin of D-rich fluids because of just preliminary results. In the future, we would examine more LL4-6 chondrites apatite grains to discuss the origin of extremely D-rich fluids.

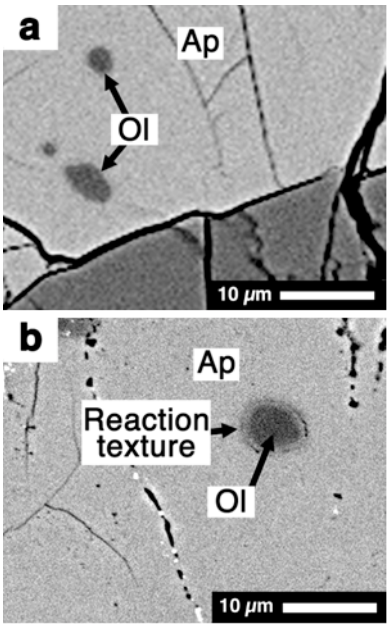

Fig.4. BSE images of olivine grains enclosed by apatite. a) Mocs apatite, b) Ensisheim apatite. Reaction texture is white area in the rim of olivine grains.

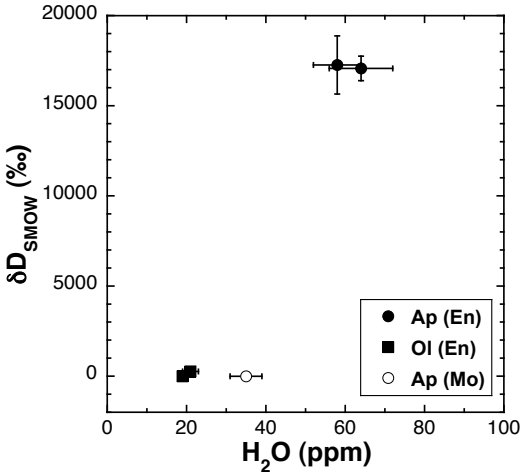

Fig. 5. H_2O contents and δD in chlorapatite determined by SIMS. Ap; apatite, Ol; olivine, En; ensisheim, Mo; Mocs.

References:

[1] Li et al. (2000) *Meteorit. Planet. Sci., 45, 135-156* [2] Dunn T. et al. (2010) *Meteorit. Planet. Sci., 35,* 561-568. [3] Jones R. H. et al. (2011) *LPSC XLII,* #2464. [4] Dreeland and Jones (2011) *LPSC XLII,* #2523. [5] Yurimoto et al. (1989) *Geochim. Cosmochim. Acta* ***53,*** 751. [6] Kurosawa et al. (1997) *Phys. chem. minerals* **24**, 385. [7] Greenwood et al. (2011) *Naturegeoscience* **4**, 79. [8] Suzuoki and Epstein (1976) *Geochim. Cosmochim. Acta* ***40,*** *1229.*